

Distinguishing the monomer to cluster phase transition in concentrated lysozyme solutions by studying the temperature dependence of the short-time dynamics

This article has been downloaded from IOPscience. Please scroll down to see the full text article.

2012 J. Phys.: Condens. Matter 24 064114

(<http://iopscience.iop.org/0953-8984/24/6/064114>)

View [the table of contents for this issue](#), or go to the [journal homepage](#) for more

Download details:

IP Address: 129.6.122.135

The article was downloaded on 25/06/2012 at 19:20

Please note that [terms and conditions apply](#).

Distinguishing the monomer to cluster phase transition in concentrated lysozyme solutions by studying the temperature dependence of the short-time dynamics

Péter Falus¹, Lionel Porcar¹, Emiliano Fratini², Wei-Ren Chen³, Antonio Faraone^{4,5}, Kunlun Hong⁶, Piero Baglioni² and Yun Liu^{4,7}

¹ Institut Laue-Langevin, BP 156, F-38042 Grenoble CEDEX 9, France

² Department of Chemistry and CSGI, University of Florence, Florence, I-50019, Italy

³ NSS Division, Spallation Neutron Source, Oak Ridge National Laboratory, Oak Ridge, TN, 37831, USA

⁴ Center for Neutron Research, National Institute of standards and Technology, Gaithersburg, MD, USA

⁵ Department of Materials Science and Engineering, University of Maryland, College Park, MD, USA

⁶ Center for Nanophase Materials Sciences, Oak Ridge National Laboratory, Oak Ridge, TN, USA

⁷ Department of Chemical Engineering, University of Delaware, Newark, DE, USA

E-mail: yunliu@nist.gov

Received 29 April 2011, in final form 25 July 2011

Published 25 January 2012

Online at stacks.iop.org/JPhysCM/24/064114

Abstract

Recent combined experiments by small angle neutron scattering (SANS) and neutron spin echo (NSE) have demonstrated that dynamic clusters can form in concentrated lysozyme solutions when the right combination of a short-ranged attraction and a long-ranged electrostatic repulsion exists. In this paper, we investigate the temperature effect on the dynamic cluster formation and try to pinpoint the transition concentration from a monomeric protein phase to a cluster phase. Interestingly, even at a relatively high concentration (10% mass fraction), despite the significant change in the SANS patterns that are associated with the change of the short-ranged attraction among proteins, the normalized short-time self-diffusion coefficient is not affected between 5 and 40 °C. This is interpreted as a lack of cluster formation in this condition. However, at larger concentrations such as 17.5% and 22.5% mass fraction, we show that the average hydrodynamic radius increases significantly and causes a large decrease of the normalized self-diffusion coefficient as a result of cluster formation when the temperature is changed from 25 to 5 °C.

 Online supplementary data available from stacks.iop.org/JPhysCM/24/064114/mmedia

(Some figures in this article are in colour only in the electronic version)

1. Introduction

Although colloid particles in a solution are dispersed randomly without a seemingly obvious long-ranged structure like that in a crystal, they can form a relatively short-ranged ordering that is determined by their interaction potentials [1].

These structural arrangements in a solution determine their macroscopic properties such as viscosity, osmotic compressibility, gelation/glass transition and spontaneous patterning [2–5]. Therefore, the study of the structure in a colloidal solution has been very active as colloidal suspensions are very common in many pharmaceutical/chemical industrial processes.

On the other hand, the structural understanding of colloidal dispersions in solution is very challenging due to their apparently random distribution. Statistical mechanics theories have been widely applied to interpret the experimental data obtained by different techniques such as dynamic light scattering [6], static light scattering [7], neutron/x-ray scattering [8–11], and confocal microscopy [3, 12]. In order to understand the structure of colloidal suspensions, many efforts have been devoted to carefully describing the so-called inter-particle structure factor, $S(Q)$, and the pair distribution function, $g(r)$ [13, 14]. It is well known that $S(Q)$ and $g(r)$ are directly linked with each other. The details of the relation between $S(Q)$ and $g(r)$ and how to calculate them by solving the Ornstein–Zernike equation with different closure forms have already been studied in many papers for decades [13, 14]. On the other hand, $S(Q)$ can be extracted experimentally from small angle neutron (SANS)/x-ray (SAXS) scattering data [8–10, 15].

Very interestingly, recent research experiments have identified that when a colloidal system interacts with both a short-ranged attraction and a long-ranged repulsion, there can form an intermediate range order (IRO) structure that is typically associated with a low Q peak in SANS/SAXS patterns which is called an IRO peak [16]. Here Q is the transferred wave vector associated with a scattering experiment. Different kinds of IRO structures can be formed depending on the inter-particle potentials [16]. Among them, one of the recent interests is the formation of dynamic clusters at very high concentrations [16–18].

Using a confocal microscope, researchers have observed the formation of clusters in poly(methyl methacrylate) (PMMA) particle solution despite the existence of the long-ranged repulsion [12]. The short-ranged attraction in this kind of system is tuned by adding non-adsorbing polymers to the solution [19]. When the attraction strength is strong enough, equilibrium clusters can be formed in solutions [12, 20, 21]. The PMMA particles can form one-dimensional rods and eventually percolate through the system to become a gel [12]. Molecular dynamic (MD) simulations have confirmed these observations too [22]. However, for much smaller particles such as lysozyme proteins, the existence of equilibrium clusters in solutions was quite controversial [17, 23–25] until a combined study using both SANS and neutron spin echo (NSE) demonstrated that at relatively low concentrations there are no clusters in lysozyme solutions and at very high concentrations dynamic clusters can form [18]. The short-time diffusion coefficient, D_s , was studied as a function of concentration at room temperature. The authors also found that when particles form clusters, the self-diffusion coefficient is dramatically slowed down as the proteins have to move together in a cluster.

In PMMA solutions, the attraction strength is altered by changing the polymer concentration so that the cluster size is increased and eventually the system becomes a gel [26]. In this paper, we wish to tune the attraction strength among lysozyme proteins by changing temperature and subsequently to monitor the effect of temperature on both the D_s and the apparent hydrodynamic radius. We define a system without

clusters as a monomer phase and a system where clusters dominate as a cluster phase. We, therefore, would like to find the transition concentration from a monomer phase to a cluster phase through investigation of the temperature dependence of the self-diffusion coefficient. Previously, we have identified the monomer phase at very low concentration and the cluster phase at very high concentration by calculating the average hydrodynamic radius based on an approximated theory [18]. It is not clear whether a sample should be in a cluster phase or a monomer phase for concentrations between the two extreme cases when the calculated average hydrodynamic radius is not very large. In this paper, we show that by studying the temperature dependence effect, we can identify the monomer phase and cluster phase unambiguously even in these intermediate conditions.

2. Experiments

Lysozyme protein and HEPES were purchased from Sigma-Aldrich⁸. The catalog numbers are L7651 and H3375 for lysozyme and HEPES respectively. The buffer solution with 20 mM HEPES was first prepared by dissolving the right amount of HEPES and then titrating with NaOH/D₂O solution to a final pD of about 7.8. Protein solutions were prepared by directly dissolving lysozyme powder into buffer solutions without further purification. 10% mass fraction, 17.5% mass fraction, 22.5% mass fraction and 25% mass fraction lysozyme proteins were prepared. SANS and NSE experiments were performed at NG3 and NG5 at the **National Institute of Standards and Technology Center for Neutron Research (NCNR)** in the USA, and D22 and IN15 at Institut Laue–Langevin in France. A detailed description of the instrumental setup of both the NSE and SANS experiments can be found elsewhere [16, 18, 27].

3. Theoretical background

In a colloidal solution, there are motions of both solute particles and solvent molecules that involve the dynamics in a wide range of time scales. Because the solvent molecules are typically so small that they move much faster than the colloidal particles, the solvent molecules can be considered to be in the equilibrium conditions at the time scale in which the diffusion of a colloidal particle is measurable. A colloidal particle's dynamics depend on several factors like interaction potentials, concentration, solution viscosity, and also the characteristic particle diffusion time, t [14]. Generally, when $\tau_B \ll t \ll \tau_I$, a colloidal particle is considered to be at the short-time limit. Here, τ_B is the momentum relaxation time [14], and τ_I is the structural relaxation time that can be expressed as

$$\tau_I = \frac{R_0^2}{D_0}, \quad (1)$$

⁸ Certain commercial equipment, instruments, or materials are identified in this document. Such identification does not imply recommendation or endorsement by the National Institute of Standards and Technology nor does it imply that the products identified are necessarily the best available for the purpose.

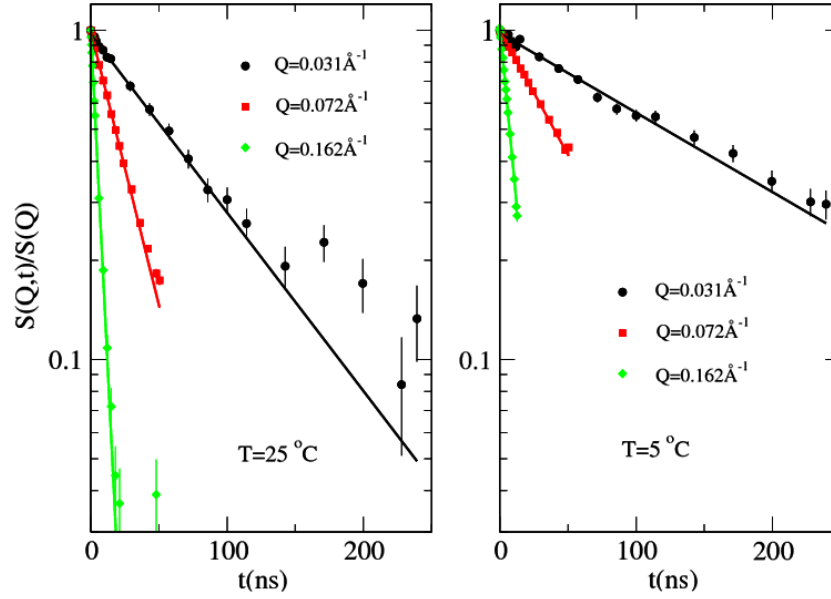


Figure 1. The intermediate scattering function is measured by NSE for 10% mass fraction lysozyme solution at 5 and 25 °C. The solid straight line is the fitting with one exponential function. The vertical lines indicate the error bars with one standard deviation.

where R_0 is the radius and D_0 is the diffusion coefficient of the colloidal particle at infinite dilution [14]. At the short-time limit, the intermediate scattering function, $S(Q, t)$, can be expressed as

$$S(Q, t)/S(Q) = e^{-Q^2 D_c(Q)t}, \quad (2)$$

where $D_c(Q) = D_0 \frac{H(Q)}{S(Q)}$ [6, 14, 28]. $D_c(Q)$ is called the collective diffusion coefficient and $H(Q)$ is the hydrodynamic function indicating how the particle diffusion is affected by the complicated solvent flow patterns created by the motions of the colloidal particles themselves. At the large Q limit, $D_c(Q) = D_s$, where D_s is the self-diffusion coefficient at the short-time limit.

In general, for a one-component system,

$$\frac{D_s}{D_0} = \frac{\eta_0}{\eta_\infty} C(\phi), \quad (3)$$

where η_∞ is the high frequency limit of the solution viscosity at volume fraction ϕ , and η_0 is the solvent viscosity. $C(\phi)$ is the correction term showing the deviation from the generalized Stokes–Einstein relation [28, 29]. Through D_s , the apparent hydrodynamic radius, R_h , can be extracted as

$$\frac{R_h}{R_0} = \frac{D_0}{D_s} \frac{\eta_0}{\eta_\infty} C(\phi), \quad (4)$$

where R_0 is the hydrodynamic radius of an individual particle. The fine details of the reported approach can be found in [18]. The protein volume fraction, ϕ_s , is calculated using the protein density reported in the literature [30].

4. Results and discussion

NSE directly measures the normalized intermediate scattering function, $S(Q, t)/S(Q)$ [31]. Figure 1 shows the NSE results

obtained for 10% mass fraction at 5 and 25 °C at different Q values. From the data, we can immediately see that $S(Q, t)/S(Q)$ at 5 °C has a much slower decay than that at 25 °C, indicating that proteins move much slower at lower temperature. The structural relaxation time, τ_1 , can be fairly estimated by knowing that R_0 for a lysozyme monomeric protein is approximately 17 Å [32]. D_0 has been determined by dynamic light scattering to be about $10.6 \text{ \AA}^2 \text{ ns}^{-1}$ at 25 °C [18]. Hence, τ_1 is about 27 ns at 25 °C based on equation (1). At 5 °C, a particle moves much slower, τ_1 is estimated to be around 49 ns. Therefore, in order to address the dynamics in the short-time limit, only the data points with $t < 27$ ns are fitted by using equation (2) although the experimental data points extend to much longer correlation times. In the supporting information (figure S1 available at stacks.iop.org/JPhysCM/24/064114/mmedia), we have also shown data points up to only about 30 ns together with the fitting. It is important to stress here that all the experimental curves at different Q values can be fitted very well using a single exponential function. Through the fitting, the collective diffusion coefficient, D_c , can then be extracted using equation (2) with its asymptotical value at high Q being D_s .

Figure 2 shows the SANS patterns of 10% mass fraction at different temperatures. When the temperature decreases, the intensity of the main peak becomes larger and its position shifts to lower Q values that are consistent with previous observations [17, 18]. Although a peak in a SANS pattern can be due to the correlation of monomeric protein molecules for many systems interacting via hard sphere or electrostatic repulsion only, the main peak in our SANS data is actually due to the formation of the intermediate range order (IRO) structure [16]. The position of this IRO peak is roughly at $\sim 0.07 \text{ \AA}^{-1}$. The shift of the peak position and the increase of the IRO peak intensity are due to the increase

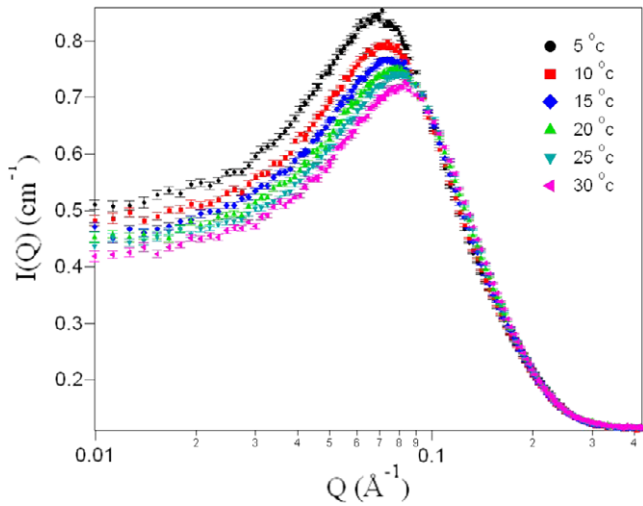


Figure 2. The SANS patterns of 10% mass fraction lysozyme solution are measured at different temperatures. The change of the scattering patterns indicates the change of the short-ranged attraction strength. The vertical lines indicate the error bars with one standard deviation.

of the short-ranged attraction as already demonstrated by theoretical calculations [16, 33]. Quite clearly, the decrease in temperature changes the solution structure significantly as indicated by the large change in the scattering patterns. It is important to point out that this IRO peak has been termed inappropriately the ‘cluster peak’ before as it was once considered to be due to the correlation of the equilibrium clusters in solutions [17, 21, 33, 34]. However, a recent study combining both SANS and NSE experiments has clearly demonstrated that the appearance of this peak can correspond to many different types of structural arrangements and is not directly related to the formation of clusters although the formation of dynamic clusters is one type of IRO structure [16].

Concurrently with the large change of the SANS patterns which indicates a large change of the colloidal structure of the sample, we might expect that the dynamics of the systems would be dramatically affected. For this reason, we have studied the temperature dependence of $D_c(Q)$, as shown in Figure 3 for the 10% mass fraction sample. The investigated Q range is from about 0.07 to 0.165 \AA^{-1} . Because we are more interested in the self-diffusion coefficient, D_s , it would be ideal to study the dynamics at even larger Q values. However, the coherent scattering intensity decreases quickly when Q increases and it would take a much longer NSE time to have a reasonable signal to noise ratio. Fortunately, it has been shown that $D_c(Q)$ normally remains almost constant for Q values larger than the IRO peak position in our cases [18]. The Q range we have chosen would be enough to extract D_s without the need to measure a sample for a very long time. When the temperature decreases, $D_c(Q)$ becomes smaller, indicating slower motions. It is very tempting to attribute the slowdown of the motions to the formation of larger clusters in solution. However, because the solvent viscosity increases when decreasing the temperature, the decrease of

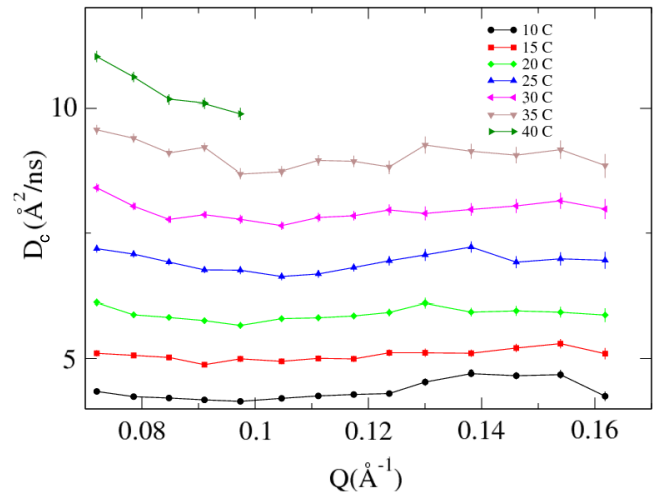


Figure 3. The collective diffusion coefficient as a function of Q is measured for the 10% mass fraction lysozyme sample at different temperatures. The vertical lines indicate the error bars with one standard deviation.

$D_c(Q)$ is partly due to the increased D_2O viscosity at lower temperatures.

One way to remove the solvent viscosity effect is to study the temperature dependence of D_s/D_0 . As both D_s and D_0 are inversely proportional to the solvent viscosity their ratio would be almost independent of the change in solvent viscosity due to the solution cooling. Since we have only measured D_0 at 25 $^\circ\text{C}$, we estimated D_0 at different temperatures by the Stokes–Einstein relation using the D_2O viscosity values present in the literature [35]. In the top panel of figure 4, D_s is estimated by averaging $D_c(Q)$ over the Q range from 0.09 to 0.16 \AA^{-1} . The estimated D_s seems to linearly increase with the temperature. It is noted that D_s at 40 $^\circ\text{C}$ may not be very accurate because there is only one point within the Q range used in the calculation. Very interestingly, D_s/D_0 remains almost constant over the entire temperature range. This is in stark contrast to the large change of SANS patterns. This means that, quite surprisingly, the large change of the colloidal structure has no effect on its normalized self-diffusion coefficient. The invariance of D_s/D_0 also implies that the average size of the moving units in the sample is not altered when the short-ranged attraction is increased by cooling down the solution. Equation (4) is used to estimate the average hydrodynamic radius at different temperatures. As expected, the normalized average hydrodynamic radius, R_h/R_0 , is essentially not affected by the temperature change.

During the estimation of R_h/R_0 using equation (4), some parameters such as η_∞/η_0 and $C(\phi)$ have to be known or assumed. However, to the best of our knowledge, there is currently no study on the generalized Stokes–Einstein relation at the short-time limit for a concentrated colloidal system with both a short-ranged attraction and a long-ranged repulsion, i.e. the corresponding η_∞/η_0 and $C(\phi)$ values are not available. The values determined for a concentrated system with only hard-sphere interaction can be used as a good approximation [18, 29]. This approach would tend to

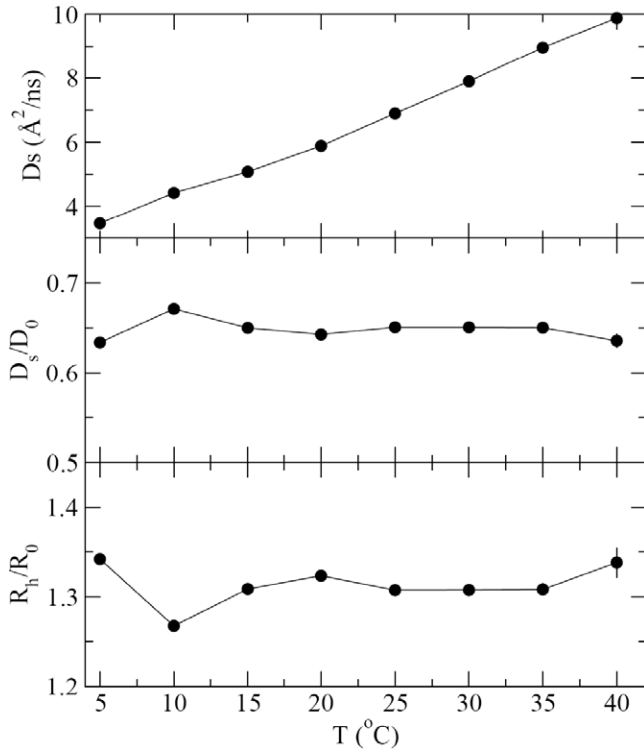


Figure 4. The top panel shows the self-diffusion coefficient extracted at different temperatures for the 10% mass fraction lysozyme sample. The middle panel shows the normalized self-diffusion coefficient. The bottom panel shows the estimated average hydrodynamic radius normalized by R_0 . The error bars are typically smaller than the symbols.

slightly overestimate the hydrodynamic radius. The obtained R_h/R_0 with this approach is about 1.3 for the 10% mass fraction sample, meaning that the real value is expected to be less than 1.3. Although we could not quantitatively quantify how much our predictions deviate from the real value, we can still determine whether there is formation of clusters at this concentration. If there is any cluster formation at one temperature in our sample, the clusters have to be formed by attractions between individual protein molecules. When decreasing the temperature, the increased attraction strength should increase the cluster size resulting in an increased hydrodynamic radius. However, at 10% mass fraction, R_h remains constant for all temperatures. Therefore, there should be no formation of dynamic clusters in this sample in all temperature ranges despite the value of R_h/R_0 being slightly larger than one. Our findings at 10% mass fraction further demonstrate that it is not appropriate to strictly rely on the features observed in static measurements such as SANS to systematically predict the formation of clusters even in a relatively large protein concentration [16, 17]. It has to be pointed out also that NSE measures the ensemble average value of a sample. Therefore, we could not exclude the possibility of a very small number of dynamic clusters in this sample even though the dominating phase is still the monomer phase.

Figure 5 shows the $D_c(Q)$ as a function of Q at 5 and 25 °C for the 10% mass fraction sample. These curves

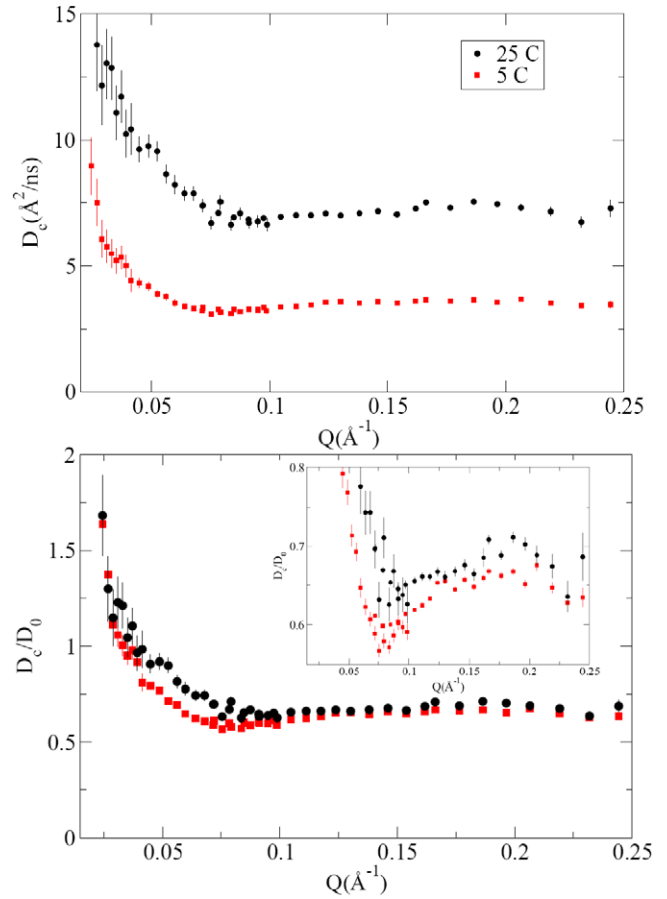


Figure 5. Top panel: the collective diffusion coefficient is obtained from NSE data as a function of Q for 10% mass fraction lysozyme solution at 5 and 25 °C. The vertical lines indicate the error bars with one standard deviation. Bottom panel: $D_c(Q)/D_0$ is plotted for the same sample at 5 and 25 °C. The inset shows that there is a small local minimum at 5 °C.

confirm the aforementioned results that $D_c(Q)$ almost remains constant once the Q value is larger than the peak position of the IRO peak. Despite the fact that D_s/D_0 has little change as a function of temperature, $D_c(Q)$ at low Q values changes dramatically. This is not surprising as $D_c(Q)$ at low Q values contains information of the mutual interaction effect because $D_c(Q) = D_0 \frac{H(Q)}{S(Q)}$. The change in SANS patterns is mostly due to the change of $S(Q)$ which will affect $D_c(Q)$. This becomes clearer in the bottom panel of figure 5, which shows $D_c(Q)/D_0$ as a function of Q . Interestingly, there seems to be a local minimum present in $D_c(Q)$ for the results at 5 °C, although it is much less clear for the results at 25 °C. The position of this small local minimum is at the Q value roughly corresponding to the IRO peak position, as is clearly shown in the inset. However, this local minimum in $D_c(Q)$ should not be interpreted as due to the narrowing effect introduced by the correlated motions between equilibrium clusters, as we have already demonstrated in figure 4 that there is no cluster formation in this sample. Due to the development of the IRO structure, the colloidal solution also has special ordering at the intermediate range length scale determined by the competition of both the short-ranged attraction and the long-ranged repulsion. From the presented experimental

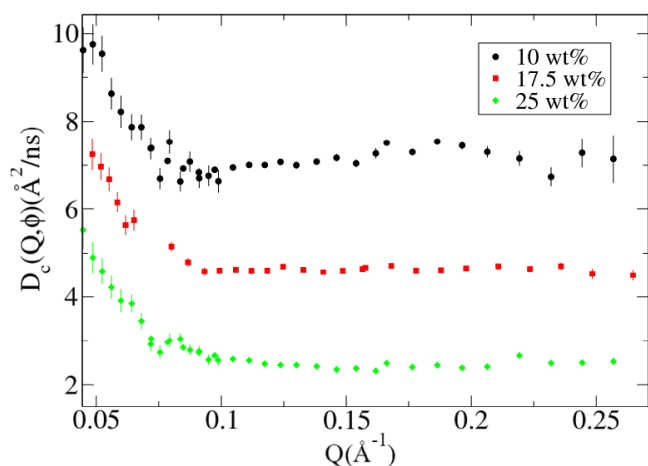


Figure 6. The collective diffusion coefficient is extracted from NSE data as a function of Q for 10%, 17.5%, and 25% mass fraction lysozyme solutions measured at 25 °C. The vertical lines indicate the error bars with one standard deviation.

results, there seems to be a characteristic motion that is also associated with this IRO structure. Given the small variation of $D_c(Q)$ for Q larger than 0.09 \AA^{-1} , this small local minimum will not have a large effect in the estimation of D_s in figure 4.

Since there are no dynamic clusters in solution at 10% mass fraction, we would thus like to study even higher concentrations to see if there is formation of dynamic clusters. Figure 6 shows the results for 10% mass fraction, 17.5% mass fraction and 25% mass fraction. In general, $D_c(Q)$ shows similar features that at relatively high Q values $D_c(Q)$ is nearly a constant. Overall, this feature is different from the results of apoferritin protein solutions and seems to be consistent with the results of myoglobin protein solutions studied also by NSE [36, 37]. For the apoferritin solutions with a small amount of salt, $D_c(Q)$ shows a very clear minimum at the Q value of the peak of $S(Q)$ when the protein concentration is about 150 mg ml^{-1} [36]. It should be noted that the interaction between apoferritin proteins in the sample is dominated by the electrostatic repulsion only without a short-range attraction as reported in [36]. Hence, the behavior of $D_c(Q)$ in apoferritin solutions is somewhat unsurprising, as in other colloidal systems with strong electrostatic repulsion $D_c(Q)$ also demonstrates a clear minimum [38]. Therefore, the lack of a clear local minimum in $D_c(Q)$ is likely associated with a strong attraction between lysozyme proteins in solutions. However, $D_c(Q)$ in myoglobin solutions seems to lack a local minimum too at the peak position of $S(Q)$. The data shown in [37] were only measured for a few points for Q values larger than the peak position. It is difficult for us to reach a conclusion by comparing our data with those in [37].

We have extracted D_s for 10% mass fraction, 17.5% mass fraction, and 25% mass fraction at 25 °C, and this is shown as green diamond symbols in the left panel of figure 7. The results obtained previously are also shown in the same figure as black squares for 5% mass fraction, 10% mass fraction, 17.5% mass fraction, and 22.5% mass fraction [18]. The new results at 25 °C for the 10% and 17.5% samples are

almost identical to the old results, indicating that the prepared samples are reproducible. Due to the limited experiment time, we could not measure all the samples at as many temperatures as for the 10% sample. Instead, we focused on obtaining the results at 5 °C and compared them with the results at 25 °C. D_s at 5 °C for 10%, 17.5%, and 22.5% is extracted and shown as red circles in the left panel of figure 7. The sample at 25% mass fraction had formed some crystals at the end of the experiment at 5 °C and, for this reason, the result was not considered. Different from the 10% mass fraction sample, D_s/D_0 decreases dramatically for the 17.5% and 22.5% samples after the temperature is dropped from 25 to 5 °C indicating that the attraction is strong enough at this high concentration to induce the formation of dynamic clusters.

The apparent hydrodynamic radius is also extracted and shown in the right panel of figure 7. The symbols in the right panel follow the same rules as those in the left panel. At 25 °C, by further increasing the concentration to 25% mass fraction, R_h/R_0 is increased to ≈ 2.7 . It is very interesting to compare the change of R_h/R_0 at different temperatures. At about 10% mass fraction, we can see that the estimated average hydrodynamic radius is almost the same when the temperature passes from 25 to 5 °C. However, it is very striking that at 17.5% and 22.5% mass fraction, R_h/R_0 increases dramatically, indicating that the average size of the moving units inside the system has increased due to the increase of attraction strength imposed by the temperature change. This conclusively confirms that at large concentrations, there is formation of dynamic clusters.

In particular, when R_h/R_0 is very large (>2), we can assume that there is cluster formation in solution. On the other hand, if the value of R_h/R_0 is very small, such as approximately one, we can safely conclude that the sample is still in a monomer phase. However, at the concentrations where R_h/R_0 is not too large, it becomes questionable as our theory may not be so accurate. Here, we show that by studying the temperature dependence, we could further identify the monomer and cluster phases when the value of R_h/R_0 itself could not help tell the solution phase of a sample. Hence we have identified that in our experimental conditions the 10% sample is a monomer-rich phase, while at higher concentrations such as 17.5% and 22.5% the samples are in cluster-rich phases.

5. Conclusions

The formation of different inter-particle structures in solution driven by both a short-ranged attraction and a long-ranged repulsion is very interesting. For PMMA particles, the equilibrium clusters have been observed directly by confocal microscope. However, due to their small size, protein molecules in solutions cannot be visualized directly. Scattering experiments have been conducted to understand the inter-particle structure in protein solutions. Although it is challenging to correctly interpret the scattering data to understand the solution structure, we have demonstrated that by combining both SANS and NSE we could identify IRO structures. It has been shown that when there is an

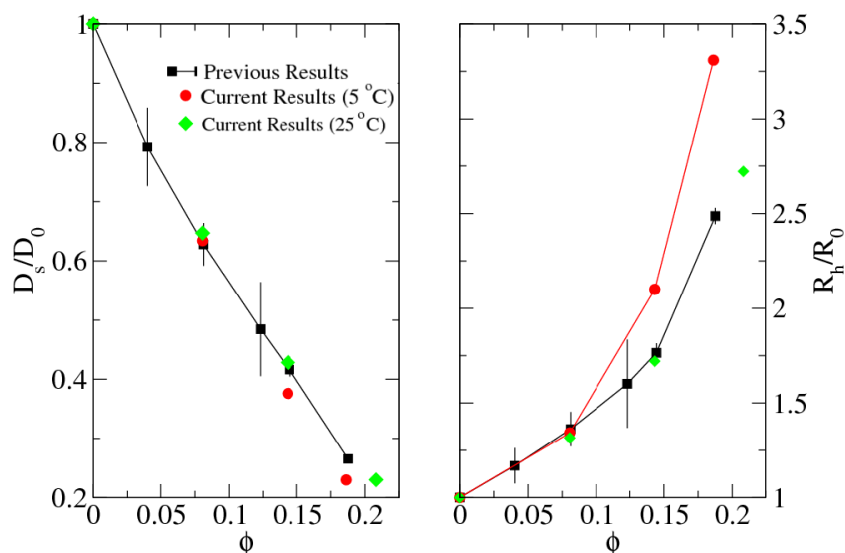


Figure 7. The left panel shows the normalized self-diffusion coefficient, D_s/D_0 , at different temperatures. The right panel shows the average hydrodynamic radius of lysozyme solutions normalized by R_0 . The black squares are the results published in [18]. The new results measured at 25 and 5 °C are shown as green diamonds and red circles in the figure. The vertical lines indicate the error bars with one standard deviation.

appropriate combination of a short-ranged attraction and a long-ranged repulsion, lysozyme proteins can form different IRO structures including dynamic clusters in concentrated solutions. In this paper, in order to find the transition concentration from a monomer phase to a cluster phase in concentrated lysozyme solutions, we have studied the temperature dependence of the short-time dynamics. We show that at 10% mass fraction, despite the large change of colloid–colloid structure in solution as shown in our SANS results, the average normalized self-diffusion coefficient is not altered by changing attraction strength as a result of the temperature variation. We have interpreted this observation as there is no formation of clusters in the solution at this concentration. The structure and dynamics are solely determined by monomeric lysozyme units despite the fact that a very intense low- Q peak (IRO peak) is evident. Although the large change of the inter-particle structure has no direct effect on its self-diffusion, the mutual diffusion coefficient at low Q values is affected dramatically by the temperature change and is more sensitive to the change of the inter-particle structures. The scenario becomes different when studying the temperature dependence of the self-diffusion coefficient at 17.5% and 22.5% mass fractions. The temperature decrease dramatically slows down the normalized self-diffusion coefficient, resulting in a much larger value of the average hydrodynamic radius for the moving units in solutions. This large change in R_h indicates that there is formation of dynamic clusters at large concentrations. Therefore, in our experimental conditions, the transition concentration from a monomer phase to a cluster phase is between 10% mass fraction and 17.5% mass fraction. Further measurements are needed to exactly locate the precise transition concentration value. Based on the present data, we have shown conclusively that at large concentrations, the formed dynamic clusters are

very sensitive to the temperature change. Our results also indicate that the cluster formation has to be studied with the support of dynamic measurements. Static measurements alone, such as SANS and SAXS, could not unambiguously tell whether there is formation of clusters in concentrated protein solutions.

Acknowledgments

This manuscript was prepared under cooperative agreement 70NANB7H6178 from NIST, US Department of Commerce. W R Chen at Spallation Neutron Source, Oak Ridge National Laboratory and K L Hong at Center for Nanophase Materials Sciences, Oak Ridge National Laboratory acknowledge the support of the Scientific User Facilities Division, Office of Basic Energy Sciences, US Department of Energy. E Fratini and P Baglioni acknowledge financial support from CSGI and MIUR (PRIN 20087K9A2J001).

References

- [1] Schaefer D W 1977 *J. Chem. Phys.* **66** 3980
- [2] Sear R P, Chung S W, Markovich G, Gelbart W M and Heath J R 1999 *Phys. Rev. E* **59** R6255
- [3] Lu P J, Zaccarelli E, Ciulla F, Schofield A B, Sciortino F and Weitz D A 2008 *Nature* **453** 499
- [4] Dekruif C G, Briels W J, May R P and Vrij A 1988 *Langmuir* **4** 668
- [5] Liu Y C, Chen S H and Huang J S 1996 *Phys. Rev. E* **54** 1698
- [6] Jones R B and Pusey P N 1991 *Annu. Rev. Phys. Chem.* **42** 137
- [7] George A and Wilson W W 1994 *Acta Crystallogr. D* **50** 361
- [8] Chen S H 1986 *Annu. Rev. Phys. Chem.* **37** 351
- [9] Chen S H, Broccio M, Liu Y, Fratini E and Baglioni P 2007 *J. Appl. Crystallogr.* **40** S321
- [10] Tardieu A, Le Verge A, Malfois M, Bonnet F, Finet S, Ries-Kautt M and Belloni L 1999 *J. Cryst. Growth* **196** 193
- [11] Hayter J B and Penfold J 1981 *Mol. Phys.* **42** 109

- [12] Campbell A I, Anderson V J, van Duijneveldt J S and Bartlett P 2005 *Phys. Rev. Lett.* **94** 208301
- [13] Caccamo C 1996 *Phys. Rep.* **274** 1
- [14] Nagele G 1996 *Phys. Rep.* **272** 216
- [15] Lonetti B, Fratini E, Chen S H and Baglioni P 2004 *Phys. Chem. Chem. Phys.* **6** 1388
- [16] Liu Y, Porcar L, Chen J, Chen W R, Falus P, Faraone A, Fratini E, Hong K and Baglioni P 2011 *J. Phys. Chem. B* **115** 7238
- [17] Stradner A, Sedgwick H, Cardinaux F, Poon W C K, Egelhaaf S U and Schurtenberger P 2004 *Nature* **432** 492
- [18] Porcar L, Falus P, Chen W R, Faraone A, Fratini E, Hong K, Baglioni P and Liu Y 2010 *J. Phys. Chem. Lett.* **1** 126–9
- [19] Crocker J C, Matteo J A, Dinsmore A D and Yodh A G 1999 *Phys. Rev. Lett.* **82** 4352
- [20] Sedgwick H, Egelhaaf S U and Poon W C K 2004 *J. Phys.: Condens. Matter* **16** S4913
- [21] Stradner A, Cardinaux F and Schurtenberger P 2006 *J. Phys. Chem. B* **110** 21222
- [22] Sciortino F, Tartaglia P and Zaccarelli E 2005 *J. Phys. Chem. B* **109** 21942
- [23] Trehwella J 2008 *Proc. Natl Acad. Sci. USA* **105** 4967
- [24] Shukla A, Mylonas E, Di Cola E, Finet S, Timmins P, Narayanan T and Svergun D I 2008 *Proc. Natl Acad. Sci. USA* **105** 5075
- [25] Shukla A, Mylonas E, Di Cola E, Finet S, Timmins P, Narayanan T and Svergun D I 2008 *Proc. Natl Acad. Sci. USA* **105** E76
- [26] Sanchez R and Bartlett P 2005 *J. Phys.: Condens. Matter* **17** S3551
- [27] Liu Y, Fratini E, Baglioni P, Chen W R and Chen S H 2005 *Phys. Rev. Lett.* **95** 118102
- [28] Banchio A J and Nagele G 2008 *J. Chem. Phys.* **128** 104903
- [29] Banchio A J, McPhie M G and Nagele G 2008 *J. Phys.: Condens. Matter* **20** 404213
- [30] Gekko K and Noguchi H 1978 *J. Agric. Food Chem.* **26** 1409
- [31] Mezei F 1980 *Neutron Spin-Echo (Springer Lecture Notes in Physics)* (Berlin: Springer)
- [32] Malfois M, Bonnete F, Belloni L and Tardieu A 1996 *J. Chem. Phys.* **105** 3290
- [33] Liu Y, Chen W R and Chen S H 2005 *J. Chem. Phys.* **122** 044507
- [34] Bomont J M, Bretonnet J L and Costa D 2010 *J. Chem. Phys.* **132** 184508
- [35] Millero F J, Dexter R and Hoff E 1971 *J. Chem. Eng. Data* **16** 85
- [36] Haussler W and Farago B 2003 *J. Phys.: Condens. Matter* **15** S197
- [37] Longeville S, Doster W and Kali G 2003 *Chem. Phys.* **292** 413
- [38] Gapinski J, Wilk A, Patkowski A, Haussler W, Banchio A J, Pecora R and Nagele G 2005 *J. Chem. Phys.* **123** 054708